Supporting Information

Charge Control of Fluorescent Probes to Selectively Target Cell Membrane or Mitochondria: Theoretical Prediction and Experimental Validation

Xiaoyan Zheng,*[a] Dong Wang,*[b] Wenhan Xu,[c] Siqin Cao,[d] Qian Peng,*[e] Ben Zhong Tang*[c]

[a]Beijing Key Laboratory of Photoelectronic/Electrophotonic Conversion Materials, Key Laboratory of Cluster Science of Ministry of Education, School of Chemistry and Chemical Engineering, Beijing Institute of Technology, Beijing 100081, China. E-mail: xiaoyanzheng@bit.edu.cn

[b]Center for AIE Research, College of Materials Science and Engineering, Shenzhen University, Shenzhen 518060, China. E-mail: wangd@szu.edu.cn

[c]Department of Chemistry, Hong Kong Branch of Chinese National Engineering Research Center for Tissue Restoration and Reconstruction, Institute of Molecular Functional Materials, The Hong Kong University of Science and Technology, Clear Water Bay, Kowloon, Hong Kong (China). E-mail: tangbenz@ust.hk

[d]Department of Chemistry, The Hong Kong University of Science and Technology, Hong Kong, P. R. China.

[e]Key Laboratory of Organic Solids, Beijing National Laboratory for Molecular Science (BNLMS), Institute of Chemistry, Chinese Academy of Sciences, Beijing 100190, P. R. China. E-mail: qpeng@iccas.ac.cn

Table of contents

1. Supplementary Computational Methods

1.1 General Setup. All MD simulations were performed using the GROMACS 5.1.5 suite of programs.[1] All quantum calculations were performed by Gaussian 16 package.[2] The force field parameters of AIEgens were built from the general amber force field.[3] The partial charges of AIEgens were obtained by restrained electrostatic potential charge fitting method[4] based on the optimized geometry at ωB97XD/6-31+G(d,p) level[5]. The AMBER Lipid14 force field[6] was used to describe the lipid POPC (Figure S1). Water molecules were described using the TIP3P model.[7] All simulations were performed under periodic boundary conditions. The temperature is coupled with the Velocity rescaling thermostat.[8] The pressure is coupled with Parrinello-Rahman barostat.[9] Especially, for bilayer related system, semi-isotropic coupling was applied such that changes of the box size in the *z*-dimension (normal of bilayer membrane) were uncoupled from the *x*- and *y*-dimensions. The coupling time of temperature and pressure are 0.1 ps and 1.0 ps respectively. The long-range electrostatic interactions were computed using particle mesh Ewald method with a real space cutoff of 1.2 nm.[10] The van der Waals interactions were calculated with a cutoff of 1.2 nm. All bond lengths were constrained by the LINCS algorithm.[11] The time step for integration is 2 fs.

1.2 Pure Lipid Membrane. The POPC bilayer membrane was built by CHARMM-GUI Lipid Builder online,[12] including a total of 144 POPC molecules (72 lipids per monolayer). The bilayer systems were placed in a rectangular box, where *z*-axis is normal to lipid bilayer and solvated by 12,157 water molecules. The system was first energy minimized by 6,000 steps by steepest descent method, followed by 500 ps MD simulations under NVT ensemble (T = 310 K) with constraints on lipids. After energy minimization, 500 ps MD simulations were performed under NVT ensemble (T = 310 K) with constraints on lipids, followed by 30 ns production simulation to fully relax the bilayer system under NPT ensemble.

1.3 AIEgen-Lipid Bilayer System. To obtain the initial structures of AIEgen-lipid bilayer system, the two AIEgens TTPy and TTVP was placed at the center of equilibrated lipid membrane by INFLATEGRO program[13] with its principle axis along the normal direction of lipid bilayer, respectively. The system was then solvated by 12,002 waters for TTPy and 12,110 waters for TTVP, and the counterions were added to keep system neutral. Then system was energy minimized by steepest descent method regularly. First, we preformed 2,000 steps energy minimization for lipids with constraints on AIEgen and waters, then 10,000 steps relaxation of waters with constraints on others, followed by 1,000 steps energy minimization with constraints only on waters, finally the whole system was fully relaxed. Initial heating from 50 K to 310 K were run for 200 ps and followed by 300 ps MD simulations under NVT ensemble with constraints on lipids and AIEgens, then we run 500 ps MD simulations under NPT ensemble with the same restraints. Finally, we performed 5 ns MD simulation under NPT ensemble removing constraints on lipids.

1.4 Pulling Simulations. Each AIEgen was then pulled from z = 0 Å (membrane center) out to 45 Å (bulk water), at pulling rate of 1 Å/ns by running 45 ns simulation under NPT ensemble with semi-isotropic scaling protocol. During the pulling simulation, a harmonic restraint of 1,000 $kJ \cdot mol^{-1} \cdot nm^{-2}$ was applied on lipids only along the z-dimension, allowing them to move freely in the x- and y-dimensions. The configurations were recorded with the time interval of 2 ps and 50,000 configurations in total were collected for each system.

1.5 Potential of Mean Force Simulations. To determine the free energy profiles of translocation, umbrella sampling techniques were used.[14] Snapshots from the pulling trajectories were selected to initiate the umbrella sampling simulations. The umbrella sampling simulations were setup by 46 windows along the normal direction of the bilayer from z = 0 Å to 45 Å, with separation between the consecutive windows 1 Å. For each window, a harmonic restraint with a force constant 1,000 $kJ \cdot mol^{-1} \cdot nm^{-2}$ were applied to the center-of-mass (COM) distance between AIEgen and lipid membrane, in the

direction normal to the bilayer surface, to ensure sampling of the entire system realized. For each window we performed 100 ns MD simulation, with the initial 20 ns for equilibration, followed by 80 ns production run. In each trajectory, the conformations and the position of AIEgen along *z*-direction were recorded with time interval of 10 and 0.1 ps, respectively. For each AIEgen, the total simulation time of the umbrella sampling simulations is 4.6 μs. The weighed histogram analysis method (WHAM)[15] were used to obtain the PMF profile. As the PMF profiles are relative, they were shifted to zero in bulk water for all cases.

1.6 Permeability Coefficients Calculations. On the basis of PMF profiles, the position-dependent diffusion, resistance and overall permeability coefficients of two AIEgens were determined through ISDM.[16] $D(z)$ is the position-dependent diffusion coefficient for AIEgen translocating along *z*-axis of lipid membrane, it is calculated by

$$D(z) = \frac{var(z)^2}{\int_0^{\infty} C_{zz}(t)dt} \tag{1}$$

Where $C_{zz}(t) = \langle \delta z(0)\delta z(t) \rangle = \frac{1}{n_{samples}} \sum_{i=0}^{n_{samples}-1} \delta z(i)\delta z(t+i)$ is the autocorrelation function of the AIEgen *z*-position in each window of the PMF calculation.[16d] It was calculated by 2 ns-block from the in total 80 ns production run of the window by integrating the $C_{zz}(t)$ curve until it had decayed to $0.01 \times var(z)$ and for each window the $D(z)$ value was averaged over 40 estimates. The position-dependent resistance $R(z)$ values were obtained by combing the $D(z)$ and the free energy profiles at each z-position, by

$$R(z) = \frac{exp^{[illegible]}(\beta \Delta G(z))}{D(z)} \tag{2}$$

Where $\beta = \frac{1}{k_B T}$, k_B is Boltzmann constant and T is temperature. The overall permeability coefficient P_{eff} can get by integration the $R(z)$ profile from the water phase in one side of the membrane $-z_b$ to the other side water phase z_b of the membrane:

$$P_{eff} = \frac{1}{R_{eff}} = \frac{1}{\int_{-z_b}^{z_b} R(z)dz} \quad (3)$$

where for both TTPy and TTVP, the integration extremes $-z_b$ and z_b equal to –45 and 45 Å, respectively.

1.7 Optical Properties Calculations. To understand the detection mechanism of fluorescent probe in living cells and provide insights on structure-property relationship at the atomistic level, the optical properties of TTVP in both lipid membrane and in dilute THF solution were investigated by the QM/MM model and polarizable continuum model (PCM), respectively. For TTVP in lipid membrane, five conformations were randomly extracted from the umbrella sampling trajectory at the window with the largest partition (z = 14 Å, Figure S7b). Centering the COM of embedded TTVP, a rectangular cutoff for lipid membrane with 40 Å in x- and y- dimensions and 90 Å in z-dimension including all relevant waters has been considered, in order to obtain the initial structures for QM/MM calculations (see Figure 3a). Only TTVP was selected as the QM region and treated by the QM method, while others in lipid membrane system were treated by the MM method. In all QM/MM models, the geometries of TTVP at both the ground and excited states were optimized by density functional theory (DFT) and time-dependent DFT at the LC-ωHPBE/6-31+G(d,p) level, respectively. For geometry optimization, all atoms in QM region were fully relaxed, while atoms in MM region were frozen. In addition, the electrostatic embedding scheme[17] was used in the QM/MM calculations. The reorganization energies of TTVP in both lipid membrane and in dilute THF solution were calculated by the isolated TTVP molecule approach using the four-point method. The radiative rate constant (k_r),

internal conversion decay rate constant (k_{IC}) and the fluorescence quantum yield (Φ_F) were obtained by MOMAP program[18] as follows.

The radiative rate constant was computed by using the spontaneous emission relationship of $k_r = \frac{1}{1.499} f \times \Delta E^2$, where f is the oscillator strength, ΔE (unit: cm^{-1}) is the energy difference between S_0 and S_1 states at the optimized geometry of S_1.

Based on the Fermi Golden Rule, the non-radiative internal conversion (IC) decay rate constant can be formulated as:

$$k_{IC} = \frac{2\pi}{\hbar} \sum_{\mu,\nu} P_{i\nu} \left| \hat{H}'_{f\mu,i\nu} \right|^2 \delta(E_{i\nu} - E_{f\mu}) \quad (4)$$

where $E_{i\nu}$ and $E_{f\mu}$ reflects the electronic and vibrational energy of the initial (final) state, $\hat{H}'$ represents the non-Born-Oppenheimer coupling.

Based on the Franck-Condon principle, applying Fourier transform of the δ-function, Eq. (4) can be written as:

$$k_{IC} = \sum_{kl} \frac{1}{\hbar^2} R_{kl} \int_{-\infty}^{\infty} dt \left[e^{i\omega_{if} t} Z_i^{-1} \rho_{IC}(t,T) \right] \quad (5)$$

where $R_{kl} = \langle \Phi_f | \hat{P}_{fk} | \Phi_i \rangle \langle \Phi_i | \hat{P}_{fl} | \Phi_f \rangle$ is the non-adiabatic electronic coupling. $\rho_{IC}(t,T)$ is the thermal vibration correlation function (TVCF),

$$\rho_{IC,kl}(t,T) = Tr\left(\hat{P}_{fk} e^{-i\tau_f \hat{H}_f} \hat{P}_{fl} e^{-i\tau_i \hat{H}_i} \right) \quad (6)$$

Then, the fluorescence quantum yield (FQY) can be obtained by:

$$\Phi_F = \frac{k_r}{k_r + k_{IC}} \quad (7)$$

Supplementary Experimental Section

2.1 Materials and Methods. Dulbecco's Modified Essential Medium (DMEM) and RPMI-1640 were purchased from Gibco (Life Technologies). Ultra pure water was supplied by Milli-Q Plus System (Millipore Corporation, United States). Phosphate buffered saline (PBS), fetal bovine serum (FBS), Cellmask Green and MitoTracker Green were purchased from Thermo Fisher Scientific. 4-(1,2,2-Triphenylvinyl)benzaldehyde and 4-(diphenylamino)benzaldehyde and piperidine were purchased from J&K or Meryer. All the chemicals used as received without further purification.

2.2 Characterization. ^{1}H spectra were measured on Bruker ARX 400 NMR spectrometers using DMSO-d_6 as the deuterated solvent. High-resolution mass spectra (HRMS) were recorded on a Finnegan MAT TSQ 7000 Mass Spectrometer System operating in a MALDI-TOF mode. UV-vis absorption spectra were taken on a Milton Ray Spectronic 3000 array spectrophotometer. Steady-state fluorescence spectra were recorded on a Perkin Elmer LS 55 spectrometer. Fluorescence images were collected on Olympus BX 41 fluorescence microscope. Laser confocal scanning microscope images were collected on Zeiss laser scanning confocal microscope (LSM7 DUO) and analyzed using ZEN 2009 software (Carl Zeiss).

2.3 Cell Culture. Cell lines were cultured in the MEM containing 10% FBS and antibiotics (100 units/mL penicillin and 100 mg/mL streptomycin) in a 5% CO_2 humidity incubator at 37 ^{o}C.

2.4 Cell Imaging. Cells were grown in a 35 mm Petri dish with a coverslip at 37 ^{o}C. The live cells were incubated with certain dye at certain concentration for certain time (by adding 2 μL of a stock solution in DMSO solution to 2 mL of cell culture medium, DMSO < 0.1 vol%). After incubation with AIEgen, in both cases of TPEPy and TPy, the cells were washed with PBS for three times; while in both cases of TPEVP and TVP, the washing procedure was not conducted. The AIEgen-labelled cells were mounted and imaged using a laser scanning confocal microscope (LSM7 DUO).

2.5 Confocal Colocalization. For co-staining with MitoTracker Green, cells were first incubated with AIEgen (TPEPy or TPy) and MitoTracker Green at 37 ^{o}C for 20 min. The medium was then removed and the cells were rinsed with PBS for three times and then imaged under confocal microscope. For TPy or TPEPy, the emission filter was 600-744 nm; for MitoTracker Green, the excitation was 488 nm and the emission filter was 490-580 nm. Moreover, for co-staining with Cellmask Green, cells were first incubated with Cellmask Green at 37 ^{o}C for 10 min, AIEgen (TPEVP or TVP) was then added into the culture, which was incubated for 1 min at room temperature. The medium was then removed and the cells were rinsed with PBS for three times and then imaged under confocal microscope. For TPEVP or TVP the emission filter was 600-744 nm; for Cellmask Green, the emission filter was 490–600 nm.

2.6 Synthetic Procedure of TPEPy. A solution of 4-(1,2,2-triphenylvinyl)benzaldehyde (72 mg, 0.2 mmol) and 1,4-dimethylpyridin-1-ium iodide (56.4 mg, 0.24 mmol) was refluxed under nitrogen in dry ethanol catalyzed by a few drops of piperidine for 24 h. After cooling to room temperature, the mixture was poured into diethyl ether. The dark red precipitates formed were filtered by suction filtration. The precipitates were re-dissolved in acetone and mixed with saturated KPF_6 solution (3 mL). After stirring for 1 h, acetone was evaporated by compressed air. The precipitates were filtered again, washed with water and dried under reduced pressure. The residue was purified by a neutral aluminum oxide column using DCM and methanol mixture (99:1 v/v) as eluting solvent to give a yellow powder of TPEPy (66.6 mg, 56% of yield). ^{1}H NMR (400 MHz, DMSO-d_6) δ 8.82 (d, J = 6.3 Hz, 2H), 8.15 (d, J = 6.3 Hz, 2H), 7.88 (d, J = 16.3 Hz, 1H), 7.51 (d, J = 7.9 Hz, 2H), 7.41 (d, J = 16.4 Hz, 1H), 7.14 (q, J = 7.2 Hz, 9H), 7.07 (d, J = 7.9 Hz, 2H), 7.00 (q, J = 7.8, 7.1 Hz, 6H), 4.23 (s, 3H). ^{13}C NMR (100 MHz, DMSO) δ 152.39, 145.48, 145.06, 142.96, 142.88, 142.72, 141.58, 140.09, 139.90, 133.26, 131.42, 130.70, 130.68, 130.60, 127.95, 127.84, 127.80, 127.62, 126.84, 126.78, 126.74, 123.40, 123.15, 46.88. ESI HRMS: calcd. for $C_{34}H_{28}N^{+}$ $[M\text{-}PF_6]^{+}$: 450.2216, found: 450.2242.

2.7 Synthesis of TPy. The synthetic process was similar to TPEPy except for the change of starting materials. Pure TPy was isolated as red powder with the yield of 79%. ^{1}H NMR (400 MHz, DMSO-d_6): ^{1}H NMR (400 MHz, DMSO-d_6) δ 8.77 (d, J = 6.5 Hz, 2H), 8.13 (d, J = 6.6 Hz, 2H), 7.93 (d, J = 16.2 Hz, 1H), 7.62 (d, J = 8.6 Hz, 2H), 7.38 (t, J = 7.8 Hz, 4H), 7.29 (d, J = 16.2 Hz, 1H), 7.19 – 7.10 (m, 6H), 6.95 (d, J = 8.6 Hz, 2H), 4.21 (s, 3H). ^{13}C NMR (100 MHz, DMSO) δ 152.80, 149.44, 146.19, 144.77, 140.49, 129.84, 129.64, 127.96, 125.39, 124.50, 122.89, 120.70, 120.45, 46.66, 40.20. ESI HRMS: calcd. for $C_{26}H_{23}N_2^+$ $[M\text{-}PF_6]^+$: 363.1856, found: 363.1876.

2.8 Synthetic Procedure of TPEVP. A solution of 4-(1,2,2-triphenylvinyl)benzaldehyde (72 mg, 0.2 mmol) and 1-(3-Trimethylammoniopropyl)-4-methylpyridinium dibromide (71 mg, 0.2 mmol) was refluxed under nitrogen in dry ethanol catalyzed by a few drops of piperidine for 24 h. After cooling to room temperature, the solvent was removed by evaporation under reduced pressure. The residue was purified by a neutral aluminum oxide column using DCM and methanol mixture (98:2 v/v) as eluting solvent to give a yellow powder of TPEVP (57 mg, 41% of yield). ^{1}H NMR (400 MHz, DMSO-d_6) δ 9.00 (d, J = 6.5 Hz, 2H), 8.26 (d, J = 6.4 Hz, 2H), 7.98 (d, J = 16.3 Hz, 1H), 7.54 (d, J = 8.0 Hz, 2H), 7.48 (d, J = 16.3 Hz, 1H), 7.15 (td, J = 7.5, 3.2 Hz, 9H), 7.07 (d, J = 8.0 Hz, 2H), 7.00 (qd, J = 7.5, 1.9 Hz, 6H), 4.59 (t, J = 7.4 Hz, 2H), 3.44 (d, J = 8.7 Hz, 2H), 3.10 (s, 9H), 2.44 (td, J = 11.9, 9.9, 5.8 Hz, 2H). ^{13}C NMR (100 MHz, DMSO) δ 153.24, 145.65, 144.45, 142.98, 142.89, 142.74, 141.64, 140.69, 139.92, 133.28, 131.45, 130.72, 130.70, 130.61, 127.99, 127.87, 127.77, 126.90, 126.82, 126.78, 123.83, 123.16, 61.79, 56.61, 52.50, 24.15.

2.9 Synthesis of TVP. The synthetic process was similar to TPEVP except for the change of starting materials. Pure TVP was isolated as red powder with the yield of 68%.^{1}H NMR (400 MHz, DMSO-d_6) δ 8.98 (d, J = 6.4 Hz, 2H), 8.21 (d, J = 6.4 Hz, 2H), 8.01 (d, J = 16.2 Hz, 1H), 7.69 – 7.59 (m, 2H), 7.37 (ddd, J = 9.6, 5.8, 2.1 Hz, 5H), 7.17 – 7.08 (m, 6H), 6.97 – 6.90 (m, 2H), 4.58 (t, J = 7.3 Hz, 2H), 3.46 (d, J = 7.6 Hz, 2H), 3.10 (s, 9H), 2.43 (d, J = 8.4 Hz, 2H). ^{13}C NMR (100 MHz, DMSO) δ 153.62,

149.58, 146.17, 144.18, 141.09, 129.88, 129.81, 127.96, 125.45, 124.58, 123.27, 120.64, 120.45, 61.81, 56.36, 52.49, 24.20.

Supplementary Figures

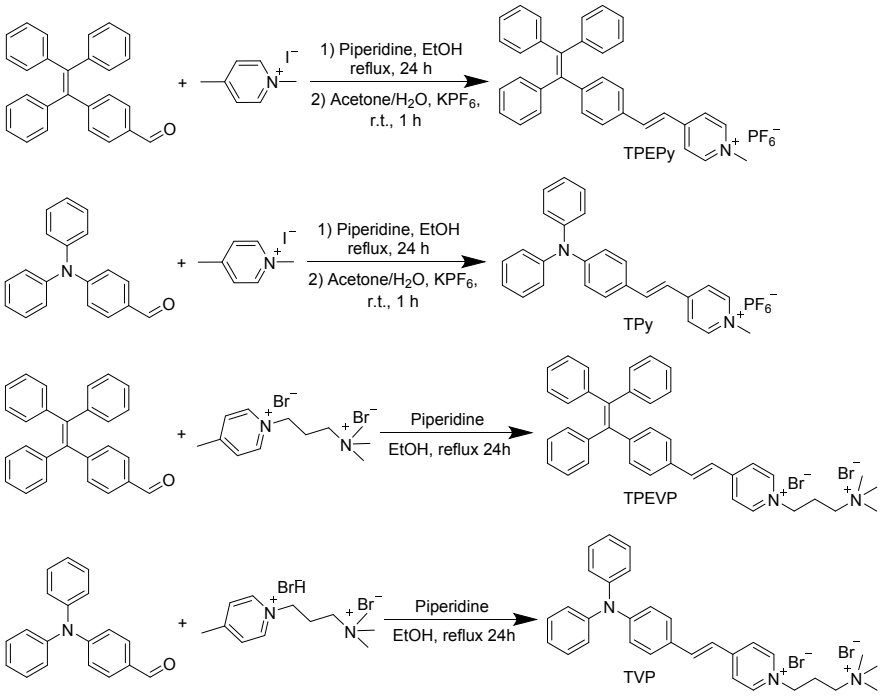

Scheme S1. Synthetic routes of new designed four AIEgens: TPEPy, TPy, TPEVP, and TVP.

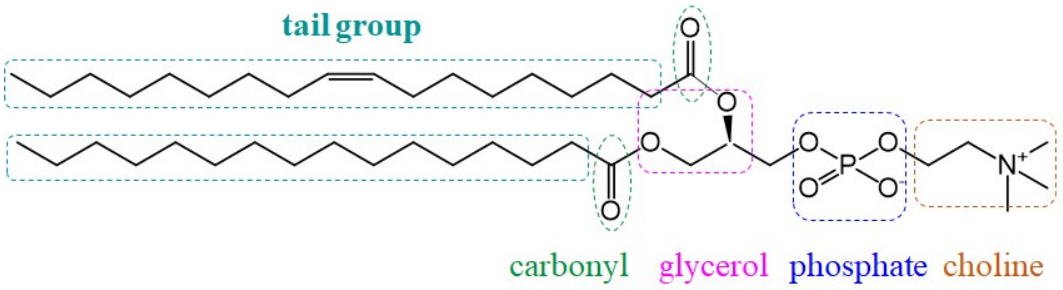

Figure S1. The molecular structure of lipid 1-palmitoyl-2-oleoyl-sn-glycero-3-phosphocholine (POPC). The tail group, carbonyl, glycerol, phosphate and choline groups of POPC are marked in cyan, green, magenta, blue and orange, respectively.

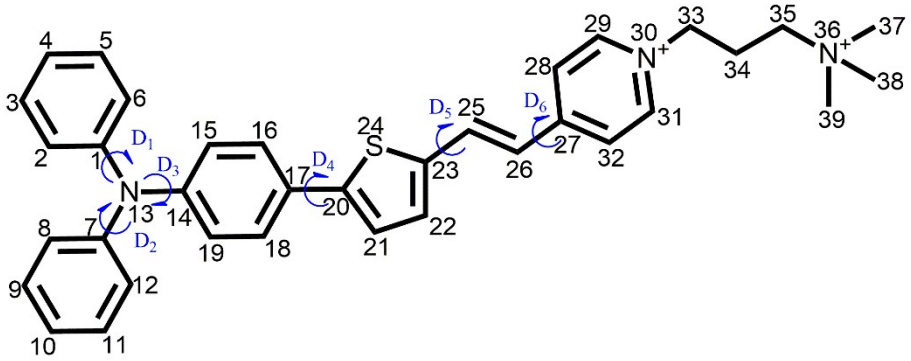

Figure S2. The molecular structure of TTVP. The key dihedral angles are highlighted by blue arrows. The atom indexes of all heavy atoms are labelled.

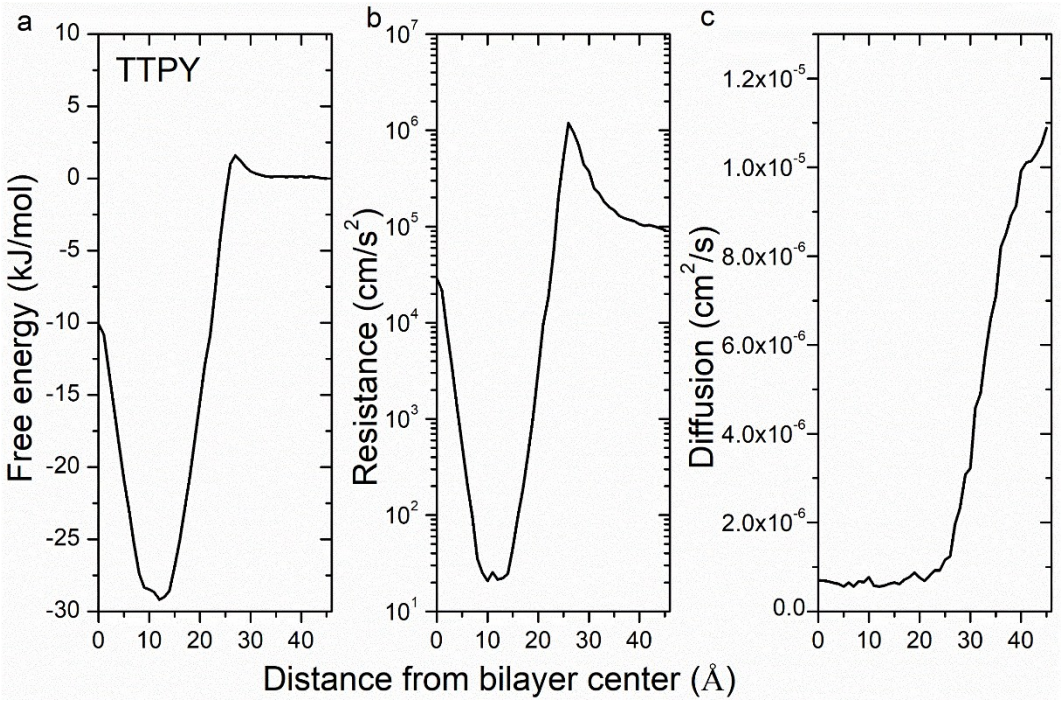

Figure S3. (a) Free energy profile, (b) resistance profile and (c) diffusion profile for TTPy transferring from bulk water into one leaflet of lipid membrane as a function of the distance between COM of TTPy and the center of lipid membrane.

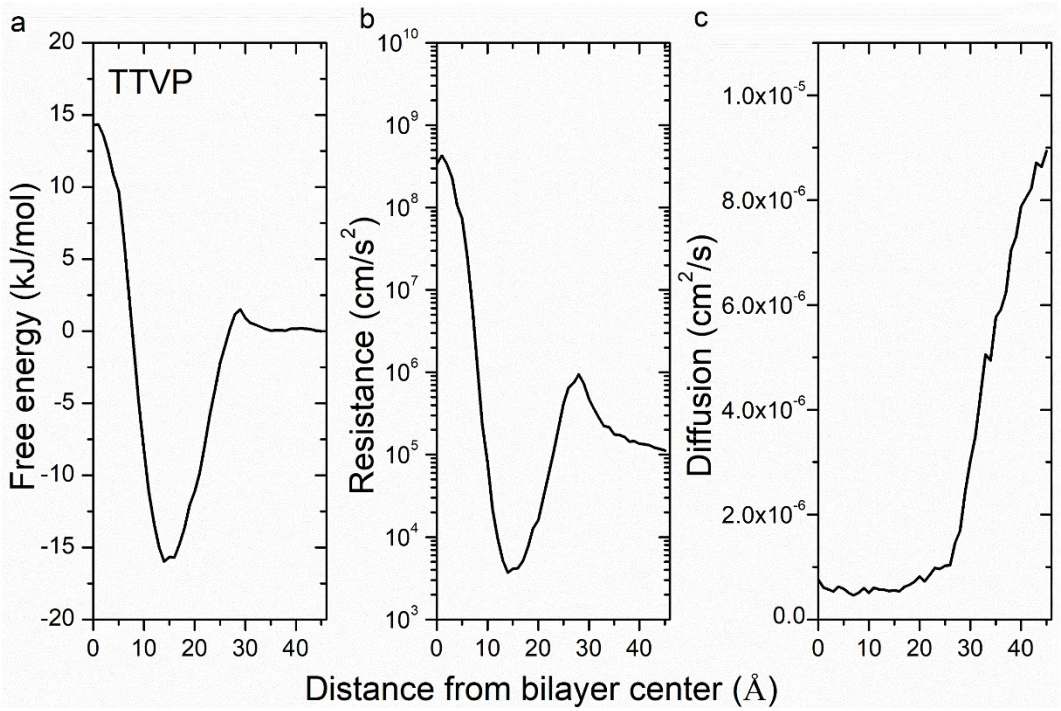

Figure S4. (a) Free energy profile, (b) resistance profile and (c) diffusion profile for TTVP transferring from bulk water into one leaflet of lipid membrane as a function of distance between COM of TTVP and the center of lipid membrane.

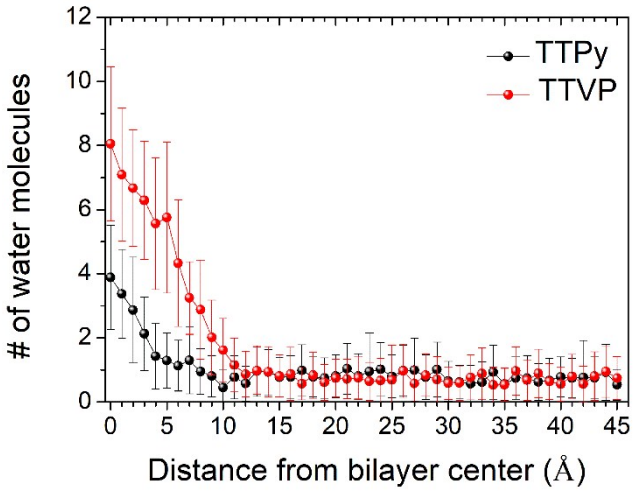

Figure S5. Number of water molecules locating in the hydrophobic core (Region I) of the lipid membrane.

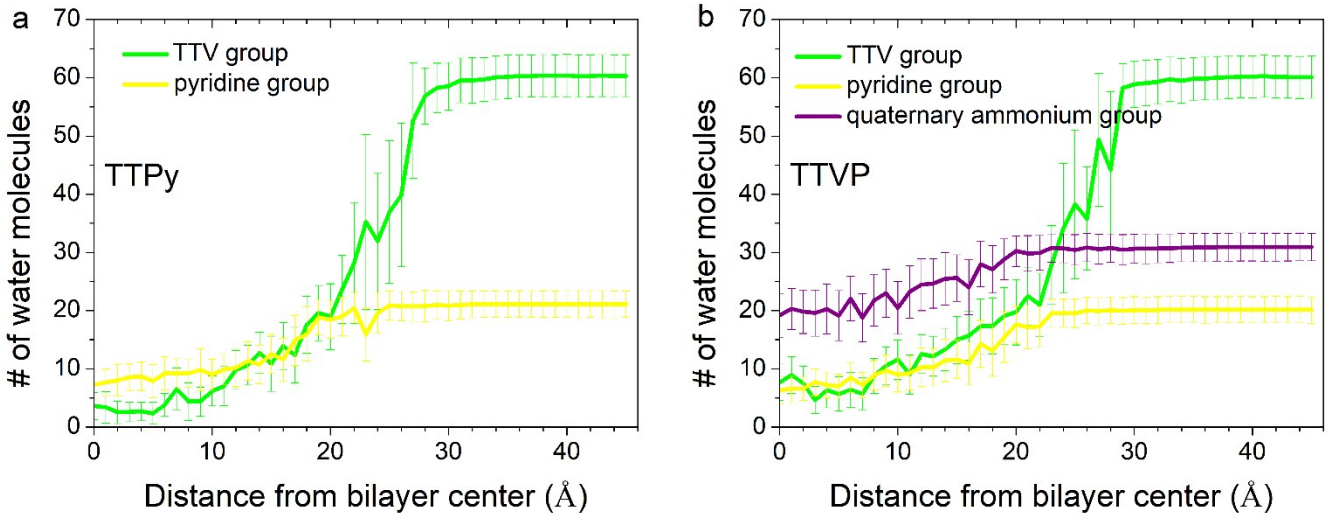

Figure S6. Number of water molecules within 10 Å of each functional group of AIEgens: (a) TTPy and (b) TTVP as a function of the distance between COM of AIEgen and the center of lipid membrane.

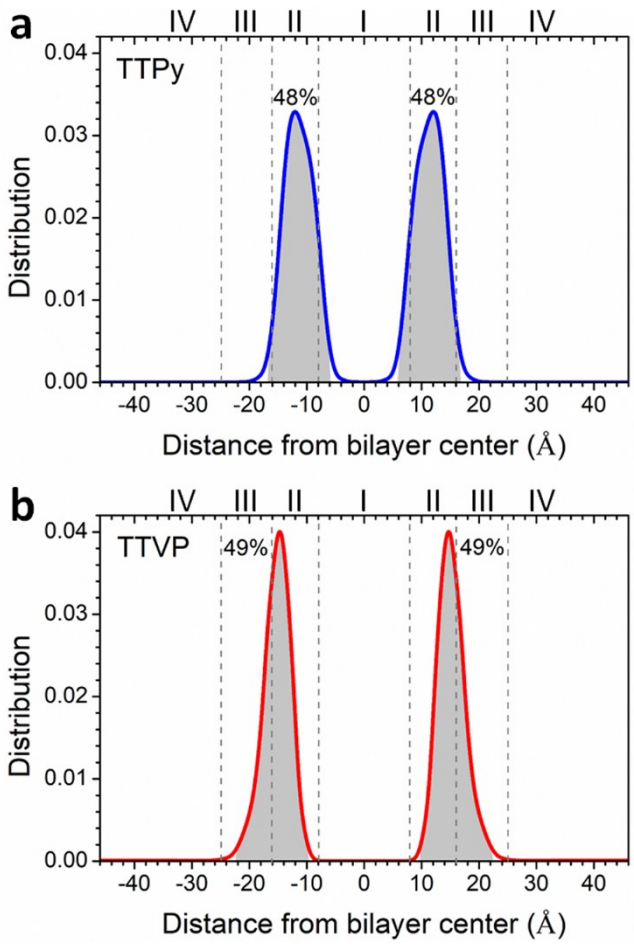

Figure S7. The partition of (a) TTPy and (b) TTVP at different *z*-position of lipid membrane obtained from PMF profiles.

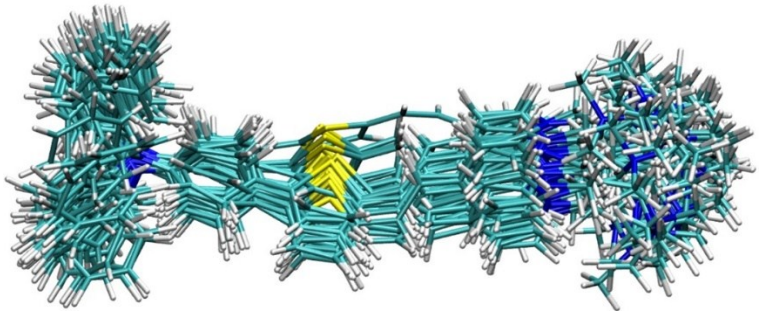

Figure S8. Align 40 conformations of TTVP in lipid membrane. The conformations were extracted from the MD trajectory of umbrella sampling simulation of TTVP at window with z = 14 Å.

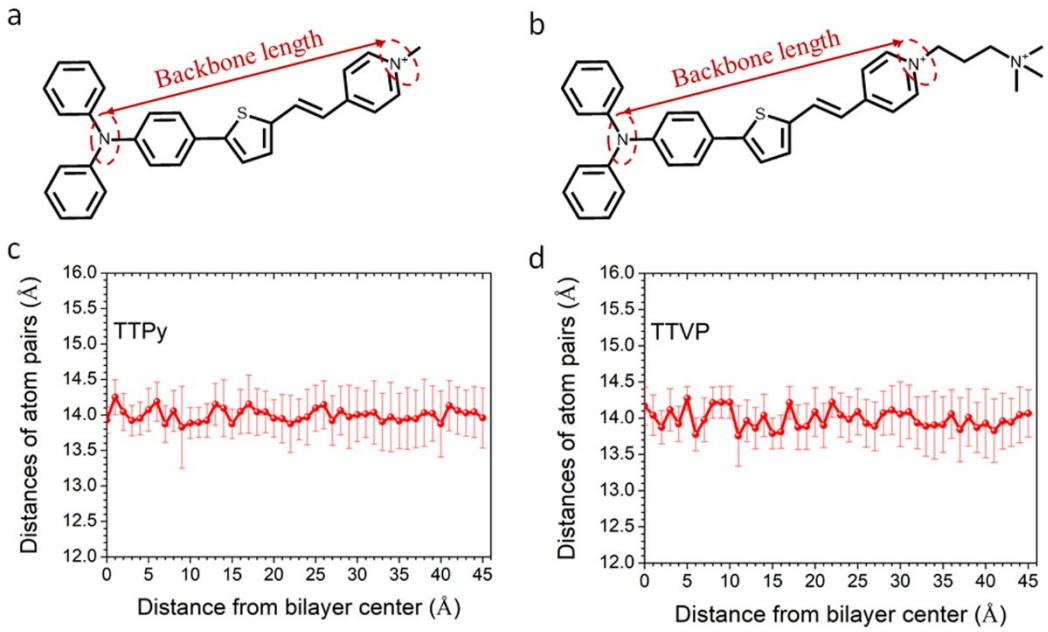

Figure S9. The label of backbone length of (a) TTPy and (b) TTVP. The average backbone length of (c) TTPy and (d) TTVP as a function of the distance between COM of AIEgen and the lipid membrane center. The standard derivation is shown in each profile.

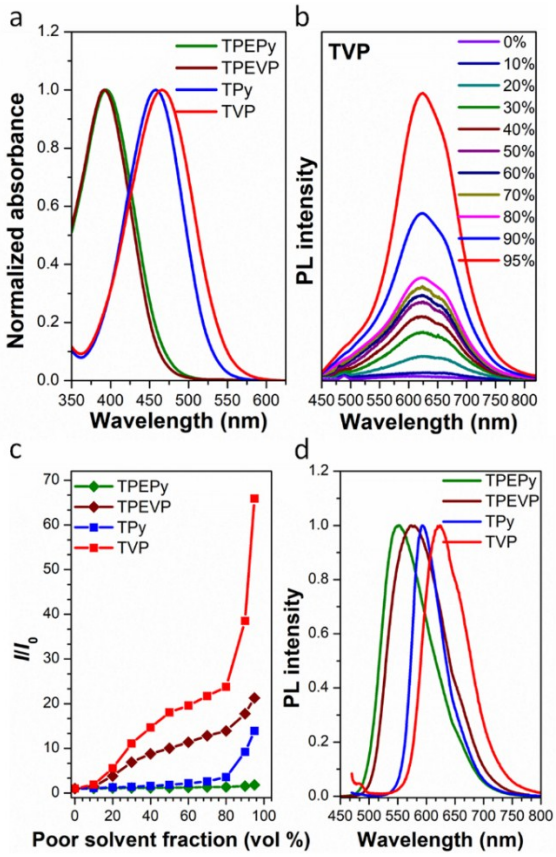

Figure S10. (a) Normalized absorption spectra of TPEPy, TPEVP, TPy and TVP in the DMSO solution. (b) PL spectra of TVP (10×10^{-6} M) in H_2O/THF mixtures with different THF fractions (f_T); λ_{ex}: 466 nm. (c) The plot of the relative emission intensity (I/I_0) versus the composition of the solvent mixture. (d) Emission spectra of these AIEgens in solid state.

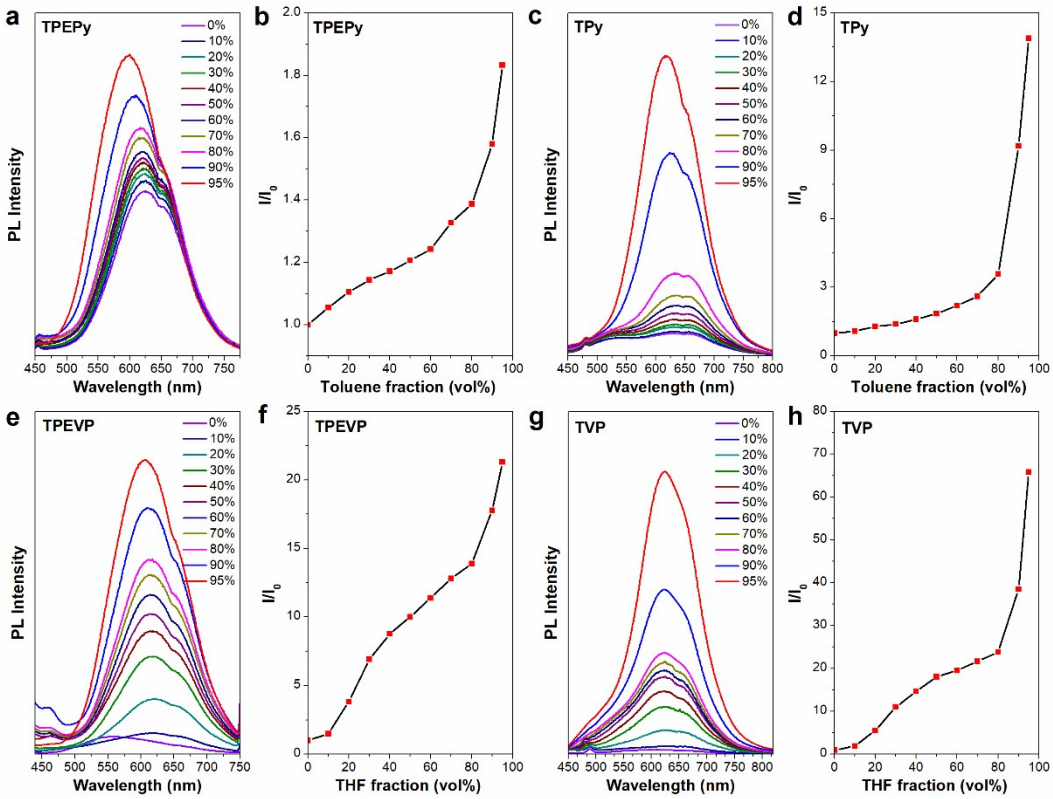

Figure S11. (a) PL spectra of TPEPy (10×10^{-6} M) in DMSO/toluene mixtures with different toluene fractions (f_T); λ_{ex}: 392 nm. (b) The plot of the relative emission intensity (I/I_0) of TPEPy versus the composition of the solvent mixture. (c) PL spectra of TPy (10×10^{-6} M) in DMSO/toluene mixtures with different toluene fractions (f_T); λ_{ex}: 394 nm. (d) The plot of the relative emission intensity (I/I_0) of TPy versus the composition of the solvent mixture. (e) PL spectra of TPEVP (10×10^{-6} M) in H_2O/THF mixtures with different THF fractions (f_T); λ_{ex}: 458 nm. (f) The plot of the relative emission intensity (I/I_0) of TPEVP versus the composition of the solvent mixture. (g) PL spectra of TVP (10×10^{-6} M) in H_2O/THF mixtures with different THF fractions (f_T); λ_{ex}: 466 nm. (h) The plot of the relative emission intensity (I/I_0) of TVP versus the composition of the solvent mixture.

2. Supplementary Tables

Table S1. The bond lengths (in Å) and dihedral angles (in degree) of the optimized structures of TTVP at both S_0 and S_1 states by the QM/MM models at LC-ωHPBE/6-31+G(d,p) level, based on the extracted five representative conformations from the umbrella sampling simulations of TTVP at window with z = 14 Å. S_0, S_1 and $|\Delta(S_1\text{-}S_0)|$ represent the geometric parameters extracted from the ground, excited state and the difference between these two states, respectively. The index of each atom is labelled in Figure S2.

index	geometric parameters	Frame 1			Frame 2			Frame 3			Frame 4			Frame 5		
		S_0	S_1	$\|\Delta(S_1\text{-}S_0)\|$	S_0	S_1	$\|\Delta(S_1\text{-}S_0)\|$	S_0	S_1	$\|\Delta(S_1\text{-}S_0)\|$	S_0	S_1	$\|\Delta(S_1\text{-}S_0)\|$	S_0	S_1	$\|\Delta(S_1\text{-}S_0)\|$
B_1	N_{13}-C_1	1.419	1.413	**0.006**	1.419	1.414	**0.005**	1.422	1.425	**0.003**	1.432	1.431	**0.001**	1.419	1.412	**0.007**
B_2	N_{13}-C_7	1.426	1.424	**0.002**	1.433	1.433	**0.000**	1.426	1.417	**0.009**	1.424	1.421	**0.003**	1.434	1.433	**0.001**
B_3	N_{13}-C_{14}	1.388	1.376	**0.012**	1.380	1.371	**0.009**	1.375	1.366	**0.009**	1.375	1.366	**0.009**	1.373	1.365	**0.008**
B_4	C_{14}-C_{15}	1.401	1.410	**0.009**	1.408	1.416	**0.008**	1.405	1.413	**0.008**	1.411	1.416	**0.005**	1.410	1.416	**0.006**
B_5	C_{15}-C_{16}	1.375	1.368	**0.007**	1.372	1.366	**0.006**	1.372	1.366	**0.006**	1.369	1.364	**0.005**	1.369	1.364	**0.005**
B_6	C_{16}-C_{17}	1.403	1.417	**0.014**	1.405	1.417	**0.012**	1.404	1.418	**0.014**	1.400	1.412	**0.012**	1.402	1.415	**0.013**
B_7	C_{17}-C_{20}	1.445	1.423	**0.022**	1.442	1.425	**0.017**	1.439	1.422	**0.017**	1.441	1.423	**0.018**	1.434	1.418	**0.016**
B_8	C_{20}-C_{21}	1.397	1.400	**0.003**	1.404	1.402	**0.002**	1.405	1.403	**0.002**	1.401	1.400	**0.001**	1.401	1.400	**0.001**
B_9	C_{21}-C_{22}	1.376	1.375	**0.001**	1.376	1.378	**0.002**	1.377	1.380	**0.003**	1.376	1.377	**0.001**	1.373	1.376	**0.003**
B_{10}	C_{22}-C_{23}	1.396	1.407	**0.011**	1.403	1.411	**0.008**	1.404	1.412	**0.008**	1.399	1.406	**0.007**	1.403	1.411	**0.008**
B_{11}	C_{23}-C_{25}	1.396	1.401	**0.005**	1.393	1.404	**0.011**	1.390	1.401	**0.011**	1.392	1.400	**0.008**	1.388	1.398	**0.010**
B_{12}	C_{25}-C_{26}	1.381	1.390	**0.009**	1.387	1.391	**0.004**	1.385	1.389	**0.004**	1.389	1.393	**0.004**	1.382	1.386	**0.004**
B_{13}	C_{26}-C_{27}	1.399	1.397	**0.002**	1.396	1.399	**0.003**	1.395	1.398	**0.003**	1.398	1.400	**0.002**	1.390	1.394	**0.004**
B_{14}	C_{27}-C_{28}	1.426	1.433	**0.007**	1.432	1.435	**0.003**	1.434	1.436	**0.002**	1.432	1.435	**0.003**	1.427	1.430	**0.003**
B_{15}	C_{28}-C_{29}	1.354	1.351	**0.003**	1.355	1.354	**0.001**	1.352	1.351	**0.001**	1.352	1.352	**0.000**	1.352	1.351	**0.001**
B_{16}	C_{27}-C_{32}	1.429	1.432	**0.003**	1.429	1.431	**0.002**	1.430	1.430	**0.000**	1.430	1.430	**0.000**	1.427	1.427	**0.000**
B_{17}	C_{31}-C_{32}	1.353	1.351	**0.002**	1.351	1.351	**0.000**	1.351	1.351	**0.000**	1.353	1.351	**0.002**	1.349	1.349	**0.000**
D_1	C_2-C_1-N_{13}-C_{14}	158.1	155.3	**2.8**	144.9	145.1	**0.2**	122.5	123.0	**0.5**	120.7	122.1	**1.4**	160.2	158.8	**1.4**
D_2	C_8-C_7-N_{13}-C_{14}	115.7	119.9	**4.2**	115.3	117.3	**2.0**	136.4	138.7	**2.3**	143.1	145.1	**2.0**	106.7	110.8	**4.1**
D_3	C_1-N_{13}-C_{14}-C_{19}	131.4	136.1	**4.7**	144.6	144.8	**0.2**	141.1	142.4	**1.3**	149.5	147.9	**1.6**	144.4	145.6	**1.2**
D_4	C_{16}-C_{17}-C_{20}-C_{21}	171.2	170.2	**1.0**	178.8	178.8	**0.0**	177.1	177.7	**0.6**	167.7	169.8	**2.1**	178.7	179.8	**1.1**
D_5	C_{24}-C_{23}-C_{25}-C_{26}	177.2	176.2	**1.0**	172.4	171.1	**1.3**	176.6	175.2	**1.4**	179.6	179.1	**0.5**	178.8	177.3	**1.5**
D_6	C_{25}-C_{26}-C_{27}-C_{32}	169.8	170.0	**0.2**	177.8	178.1	**0.3**	174.3	175.1	**0.8**	175.6	177.5	**1.9**	172.4	171.9	**0.5**

Table S2. The bond lengths (in Å) and dihedral angles (in degree) of the optimized structures of TTVP at both S_0 and S_1 states in dilute THF solution at LC-ωHPBE/6-31+G(d,p) level. S_0, S_1 and $|\Delta(S_1\text{-}S_0)|$ represent the geometric parameters extracted from the ground, excited state and the difference between these two states, respectively. The index of each atom is labelled in Figure S2.

index	geometric parameter	TTVP in dilute THF solution		
		S_0	S_1	$\|\Delta(S_1\text{-}S_0)\|$
B_1	N_{13}-C_1	1.418	1.431	**0.013**
B_2	N_{13}-C_7	1.418	1.431	**0.013**
B_3	N_{13}-C_{14}	1.403	1.361	**0.042**
B_4	C_{14}-C_{15}	1.398	1.420	**0.022**
B_5	C_{15}-C_{16}	1.384	1.363	**0.021**
B_6	C_{16}-C_{17}	1.396	1.425	**0.029**
B_7	C_{17}-C_{20}	1.469	1.402	**0.067**
B_8	C_{20}-C_{21}	1.371	1.428	**0.057**
B_9	C_{21}-C_{22}	1.414	1.361	**0.053**
B_{10}	C_{22}-C_{23}	1.372	1.432	**0.060**
B_{11}	C_{23}-C_{25}	1.443	1.380	**0.063**
B_{12}	C_{25}-C_{26}	1.345	1.410	**0.065**
B_{13}	C_{26}-C_{27}	1.452	1.395	**0.057**
B_{14}	C_{27}-C_{28}	1.405	1.436	**0.031**
B_{15}	C_{28}-C_{29}	1.367	1.356	**0.011**
B_{16}	C_{27}-C_{32}	1.404	1.435	**0.031**
B_{17}	C_{31}-C_{32}	1.369	1.354	**0.015**
D_1	C_2-C_1-N_{13}-C_{14}	135.3	125.2	**10.1**
D_2	C_8-C_7-N_{13}-C_{14}	135.6	125.7	**9.9**
D_3	C_1-N_{13}-C_{14}-C_{19}	145.6	162.6	**17.0**
D_4	C_{16}-C_{17}-C_{20}-C_{21}	152.3	177.1	**24.8**
D_5	C_{24}-C_{23}-C_{25}-C_{26}	177.7	178.6	**0.9**
D_6	C_{25}-C_{26}-C_{27}-C_{32}	175.6	177.9	**2.3**

Table S3. Calculated emission spectra, oscillator strength (*f*), the electric transition dipole moment (EDM) and the transition orbital assignments of the optimized TTVP at S_1 state for TTVP in both lipid membrane and dilute THF solution by the QM/MM model and PCM model at the LC-ωHPBE/6-31+G(d,p) level, respectively.

systems	emission (nm/eV)	*f*	EDM (Debye)	Assignments of S_1
TTVP in lipid membrane				
Frame 1	632 nm/ 1.961 eV	2.150	17.0	HOMO-1 → LUMO (20%) HOMO → LUMO (68%)
Frame 2	633 nm/ 1.958 eV	2.191	17.2	HOMO-1 → LUMO (18%) HOMO → LUMO (71%)
Frame 3	628 nm/ 1.975 eV	2.189	17.1	HOMO-1 → LUMO (18%) HOMO → LUMO (71%)
Frame 4	630 nm/ 1.969 eV	2.124	16.9	HOMO-1 → LUMO (18%) HOMO → LUMO (71%)
Frame 5	632 nm/ 1.959 eV	2.1983	17.2	HOMO-1 → LUMO (19%) HOMO → LUMO (71%)
TTVP in dilute THF solution				
TTVP in THF solution	651 nm/ 1.905 eV	2.1168	16.2	HOMO-1 → LUMO (10%) HOMO → LUMO (83%)

Table S4. Reorganization energies of TTVP in both lipid membrane and dilute THF solution calculated at LC-ωHPBE/6-31+G(d,p) level by the QM/MM model and PCM model, respectively. λ_{gs}, λ_{es} and λ_{total} indicates the ground state, excited state and the overall reorganization energies, respectively.

	λ_{gs} (meV)	λ_{es} (meV)	λ_{total} (meV)
TTVP in lipid membrane			
Frame 1	71	52	123
Frame 2	49	50	99
Frame 3	62	42	104
Frame 4	27	80	107
Frame 5	117	32	149
average	**65**	**51**	**116**
TTVP in dilute THF solution			
TTVP in THF solution	212	421	633

Table S5. Calculated radiative rate constant (k_r), internal conversion decay rate constant (k_{IC}) and fluorescence quantum yield (Φ_F) of TTVP in both lipid membrane and dilute THF solution at LC-ωHPBE/6-31+G(d,p) level.

	k_r (s^{-1})	k_{IC} (s^{-1})	Φ_F
TTVP in lipid membrane			
Frame 1	3.6×10^8	/	/
Frame 2	3.6×10^8	/	/
Frame 3	3.7×10^8	/	/
Frame 4	3.6×10^8	/	/
Frame 5	3.6×10^8	/	/
TTVP in dilute THF solution			
TTVP in THF Solution	3.3×10^8	2.4×10^{10}	1.3%

Table S6. Quantum yields of synthesized AIEgens in different states.

	TPEPy	TPy	TPEVP	TVP
Solution (%)	1.02	0.57	0.15	0.34
Solid (%)	5.14	6.19	4.72	8.13

5. NMR and HRMS Spectra of AIEgens

5.1 ^{1}H NMR spectrum of TPEPy.

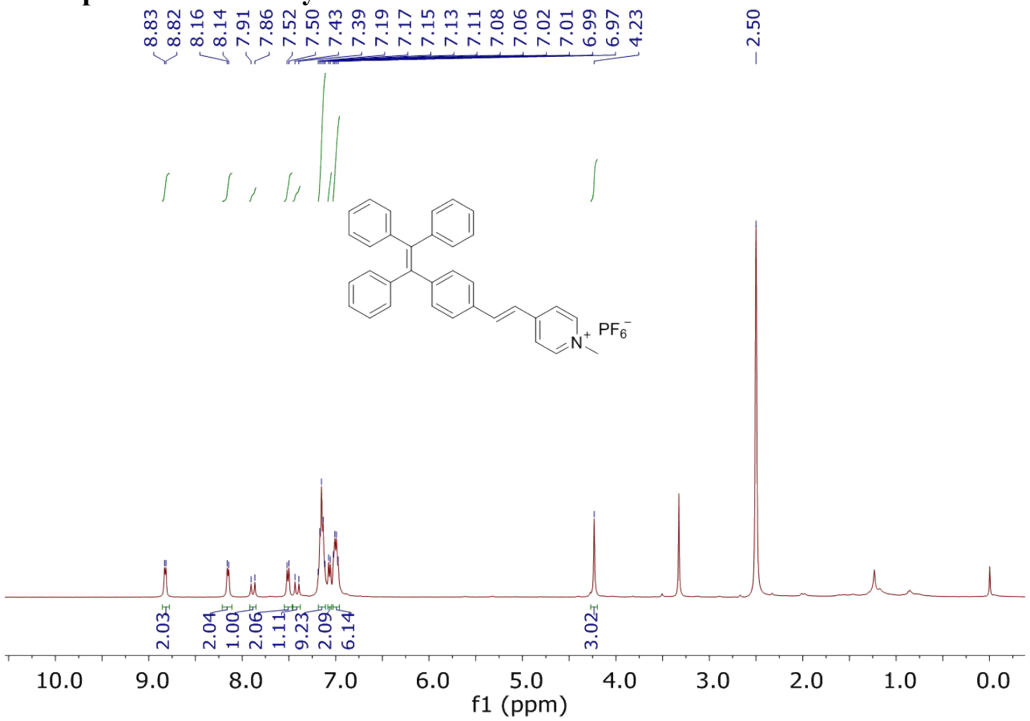

5.2 ^{13}C NMR spectrum of TPEPy.

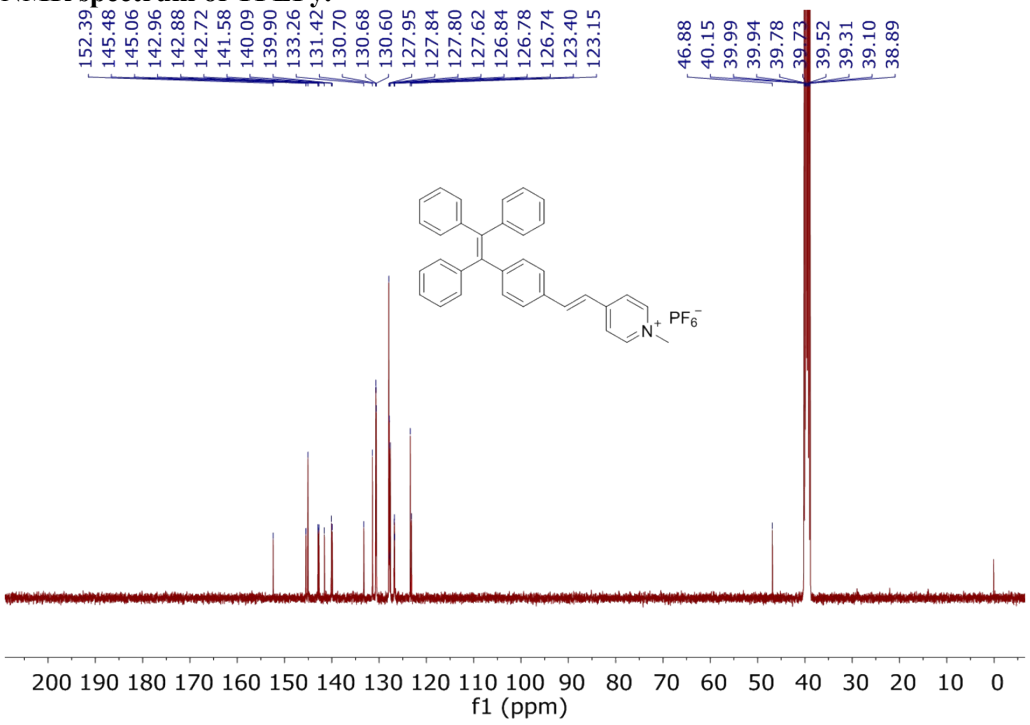

5.3 HRMS spectrum of TPEPy.

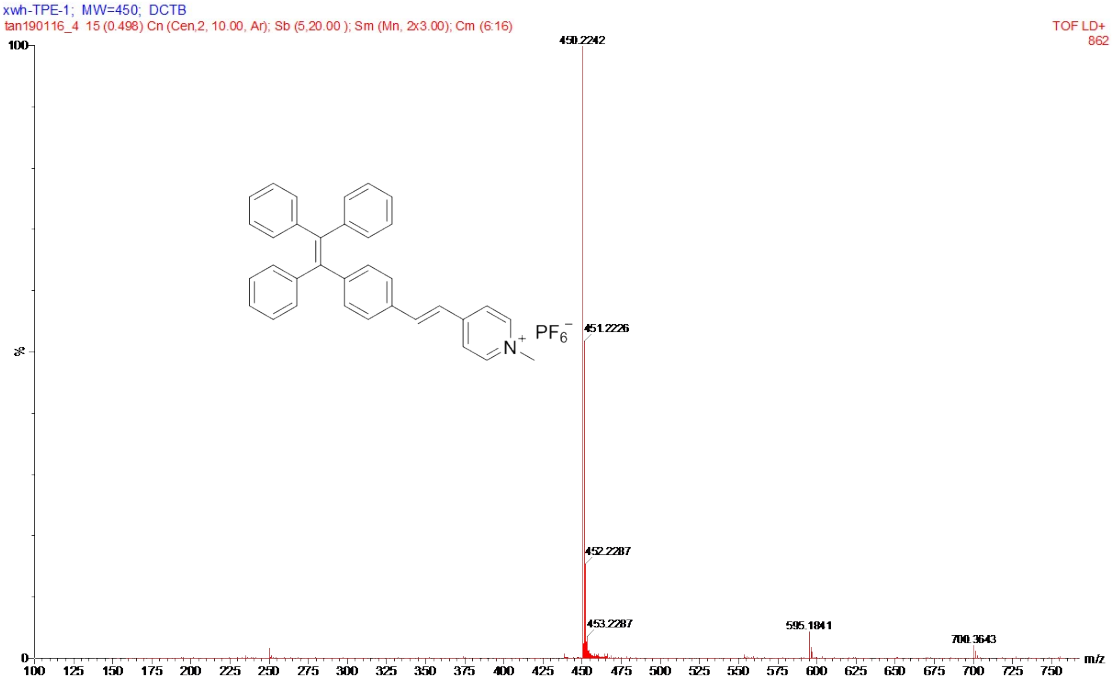

5.4 ^{1}H NMR spectrum of TPEVP

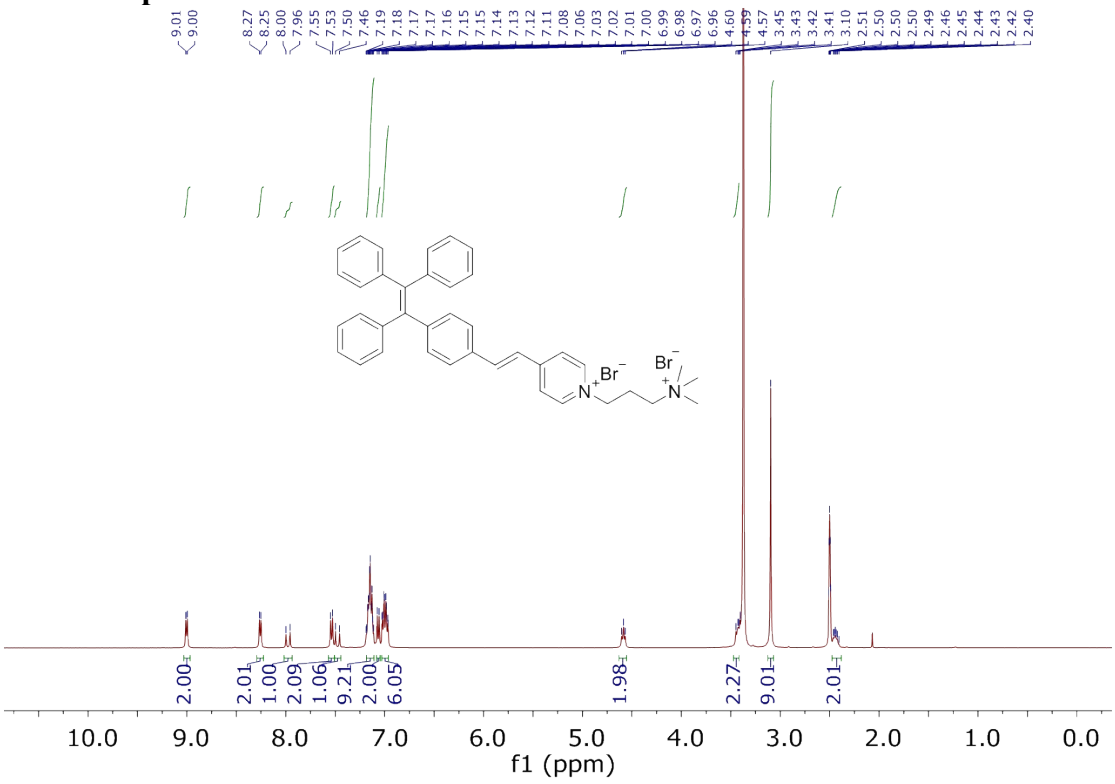

5.5 ^{13}C NMR spectrum of TPEVP

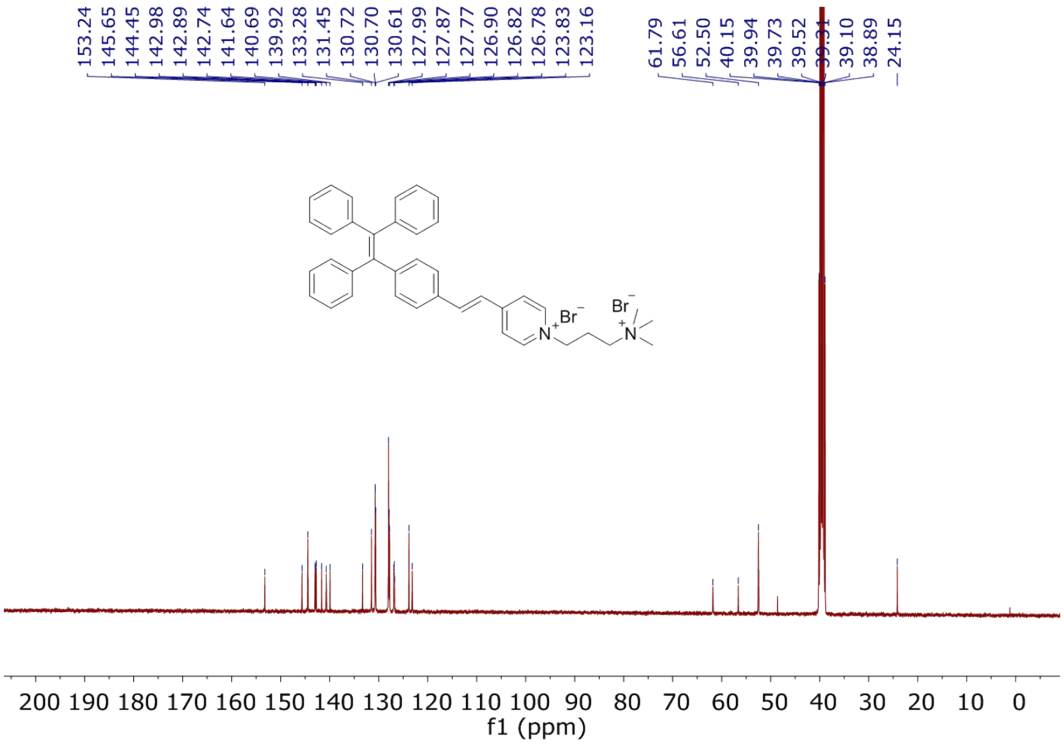

5.6 ^{1}H NMR spectrum of TPy

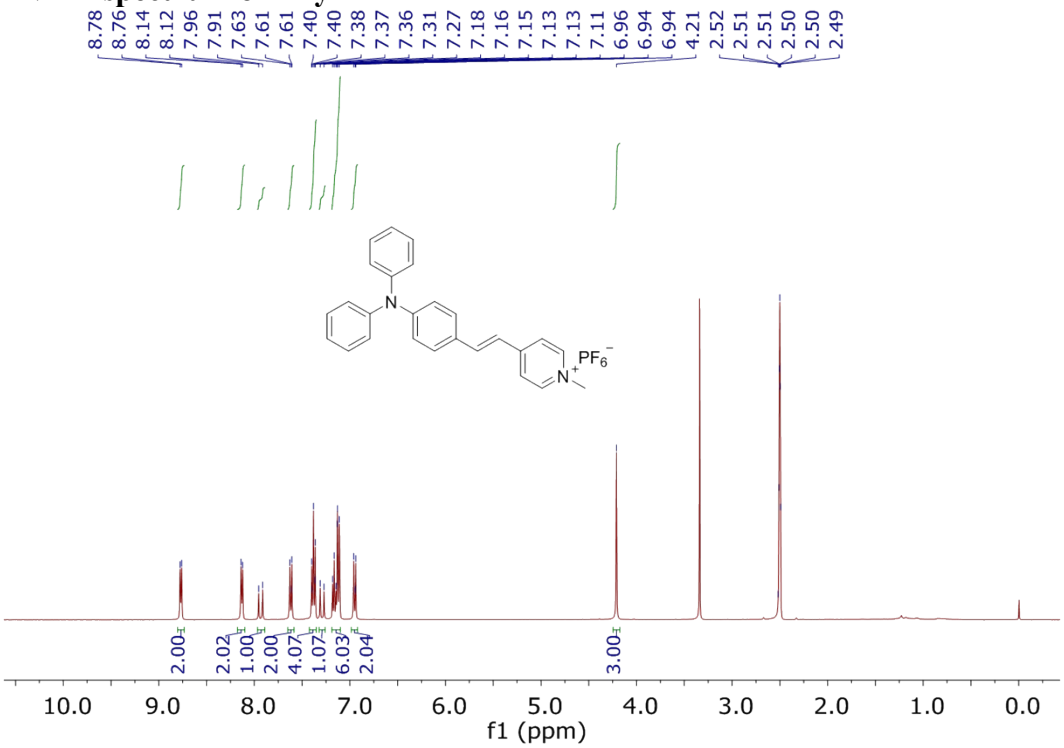

5.7 ^{13}C NMR spectrum of TPy

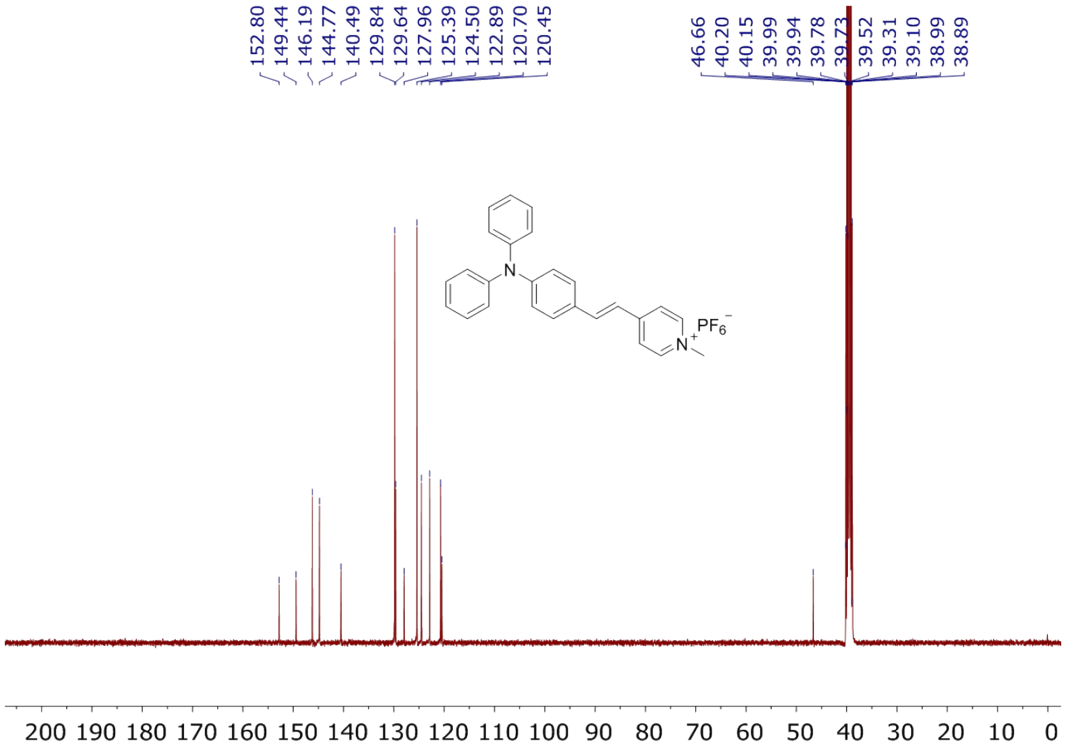

5.8 HRMS spectrum of TPy

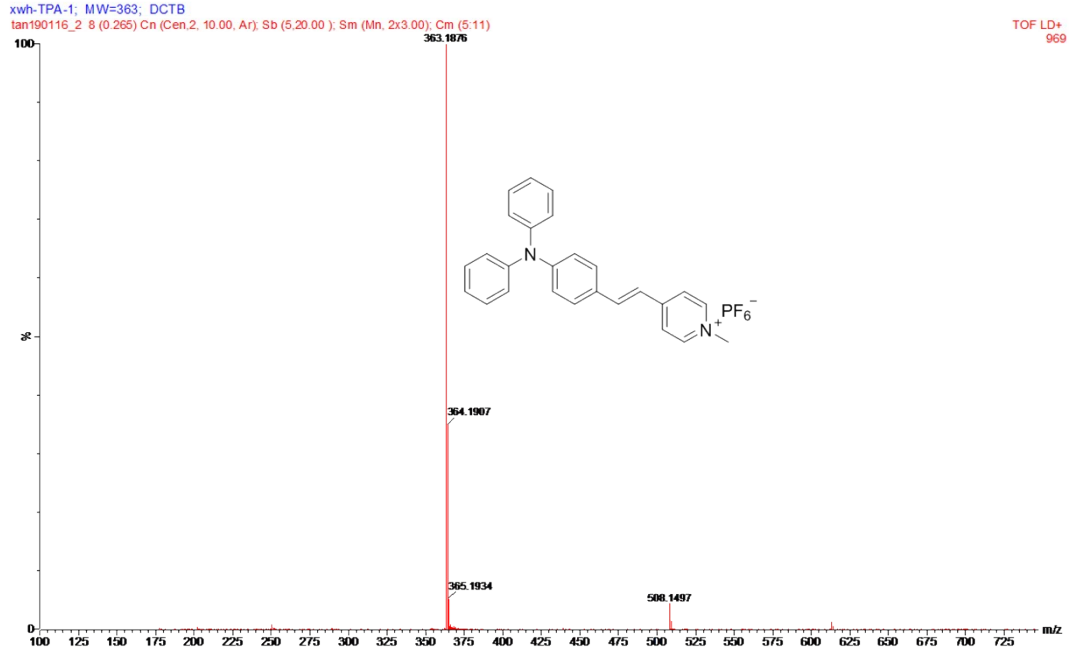

5.9 ^{1}H NMR spectrum of TVP

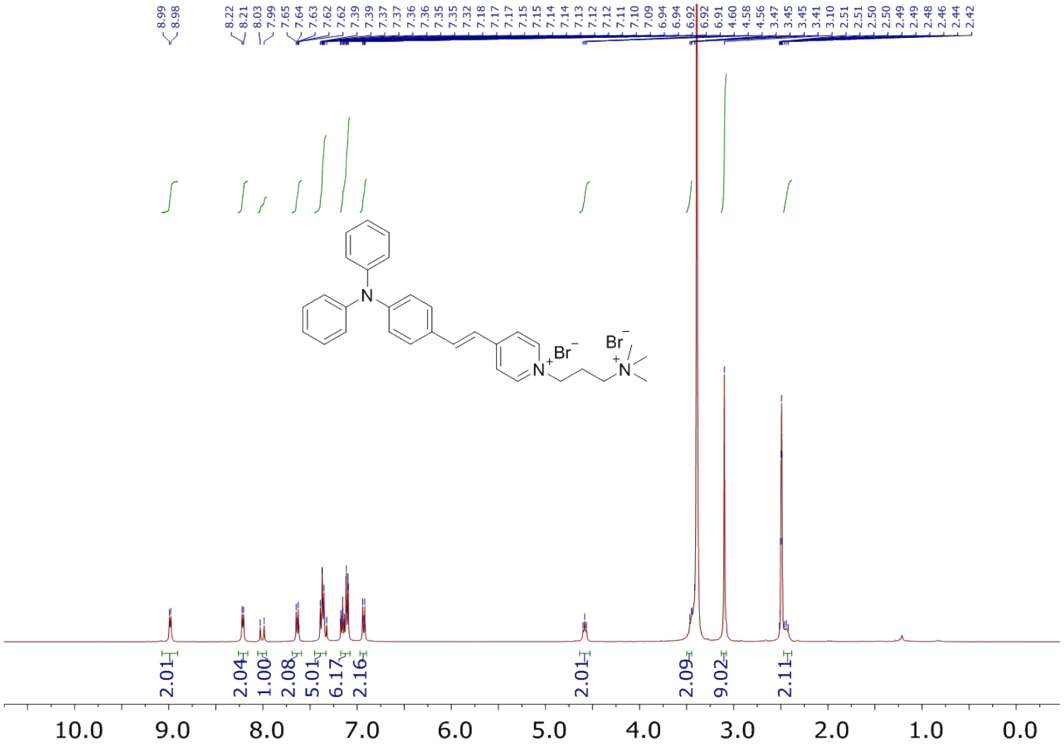

5.10 ^{13}C NMR spectrum of TVP

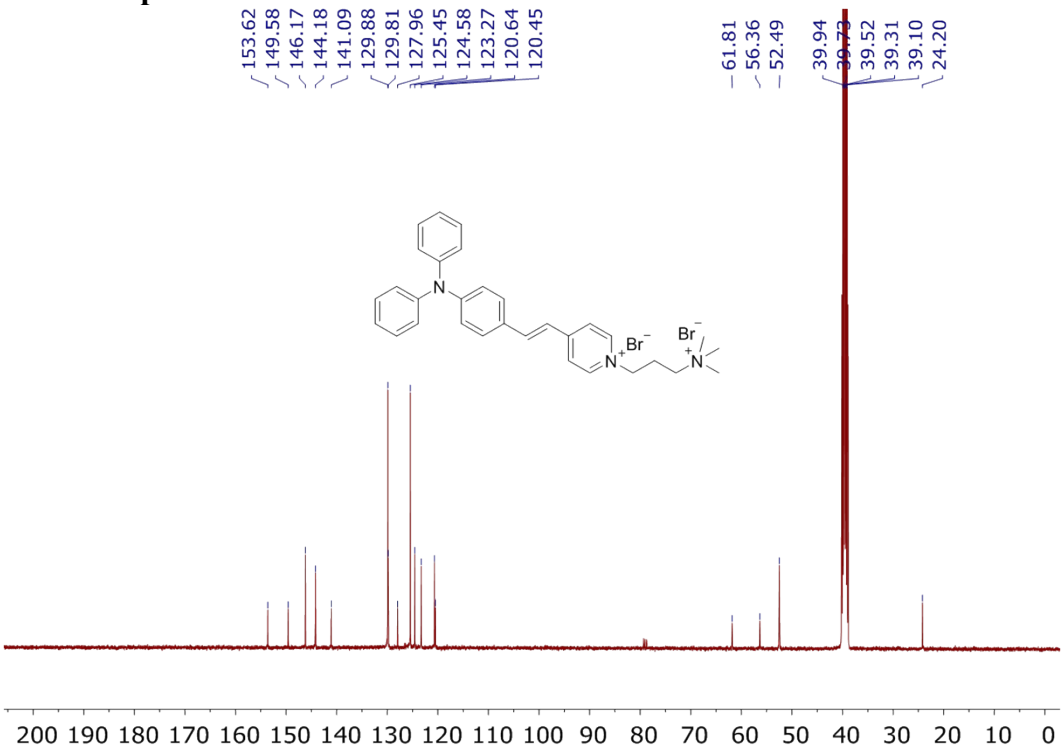

References

[1] D. Van Der Spoel, E. Lindahl, B. Hess, G. Groenhof, A. E. Mark, H. J. C. Berendsen, *J. Comput. Chem.* 2005, **26**, 1701-1718.

[2] M. J. Frisch, G. W. Trucks, H. B. Schlegel, G. E. Scuseria, M. A. Robb, J. R. Cheeseman, G. Scalmani, V. Barone, G. A. Petersson, H. Nakatsuji, X. Li, M. Caricato, A. V. Marenich, J. Bloino, B. G. Janesko, R. Gomperts, B. Mennucci, H. P. Hratchian, J. V. Ortiz, A. F. Izmaylov, J. L. Sonnenberg, Williams, F. Ding, F. Lipparini, F. Egidi, J. Goings, B. Peng, A. Petrone, T. Henderson, D. Ranasinghe, V. G. Zakrzewski, J. Gao, N. Rega, G. Zheng, W. Liang, M. Hada, M. Ehara, K. Toyota, R. Fukuda, J. Hasegawa, M. Ishida, T. Nakajima, Y. Honda, O. Kitao, H. Nakai, T. Vreven, K. Throssell, J. A. Montgomery Jr., J. E. Peralta, F. Ogliaro, M. J. Bearpark, J. J. Heyd, E. N. Brothers, K. N. Kudin, V. N. Staroverov, T. A. Keith, R. Kobayashi, J. Normand, K. Raghavachari, A. P. Rendell, J. C. Burant, S. S. Iyengar, J. Tomasi, M. Cossi, J. M. Millam, M. Klene, C. Adamo, R. Cammi, J. W. Ochterski, R. L. Martin, K. Morokuma, O. Farkas, J. B. Foresman, D. J. Fox, Wallingford, CT, 2016.

[3] J. Wang, R. M. Wolf, J. W. Caldwell, P. A. Kollman, D. A. Case, *J. Comput. Chem.* 2004, **25**, 1157-1174.

[4] (a) W. D. Cornell, P. Cieplak, C. I. Bayly, P. A. Kollmann, *J. Am. Chem. Soc.* 1993, **115**, 9620-9631; (b) C. I. Bayly, P. Cieplak, W. Cornell, P. A. Kollman, *J. Phys. Chem.* 1993, **97**, 10269-10280.

[5] (a) J.-D. Chai, M. Head-Gordon, *Phys. Chem. Chem. Phys.* 2008, **10**, 6615-6620; (b) J.-D. Chai, M. Head-Gordon, *J. Chem. Phys.* 2008, **128**, 084106.

[6] (a) C. J. Dickson, L. Rosso, R. M. Betz, R. C. Walker, I. R. Gould, *Soft Matter* 2012, **8**, 9617-9627; (b) Å. A. Skjevik, B. D. Madej, R. C. Walker, K. Teigen, *J. Phys. Chem. B* 2012, **116**, 11124-11136; (c) C. J. Dickson, B. D. Madej, Å. A. Skjevik, R. M. Betz, K. Teigen, I. R. Gould, R. C. Walker, *J. Chem. Theory Comput.* 2014, **10**, 865-879.

[7] W. L. Jorgensen, J. Chandrasekhar, J. D. Madura, R. W. Impey, M. L. Klein, *J. Chem. Phys.* 1983, **79**, 926-935.

[8] G. Bussi, D. Donadio, M. Parrinello, *J. Chem. Phys.* 2007, **126**, 014101.

[9] H. J. C. Berendsen, J. P. M. Postma, W. F. van Gunsteren, A. DiNola, J. R. Haak, *J. Chem. Phys.* 1984, **81**, 3684-3690.

[10] (a) T. Darden, D. York, L. Pedersen, *J. Phys. Chem.* 1993, **98**, 10089-10092; (b) U. Essmann, L. Perera, M. L. Berkowitz, T. Darden, H. Lee, L. G. Pedersen, *J. Chem. Phys.* 1995, **103**, 8577-8593.

[11] B. Hess, H. Bekker, H. J. C. Berendsen, J. G. E. M. Fraaije, *J. Comput. Chem.* 1997, **18**, 1463-1472.

[12] E. L. Wu, X. Cheng, S. Jo, H. Rui, K. C. Song, E. M. Dávila-Contreras, Y. Qi, J. Lee, V. Monje-Galvan, R. M. Venable, J. B. Klauda, W. Im, *J. Comput. Chem.* 2014, **35**, 1997-2004.

[13] C. Kandt, W. L. Ash, D. Peter Tieleman, *Methods* 2007, **41**, 475-488.

[14] J. Kästner, W. Thiel, *J. Chem. Phys.* 2005, **123**, 144104.

[15] S. Kumar, J. M. Rosenberg, D. Bouzida, R. H. Swendsen, P. A. Kollman, *J. Comput. Chem.* 1992, **13**, 1011-1021.

[16] (a) S.-J. Marrink, H. J. C. Berendsen, *J. Phys. Chem.* 1994, **98**, 4155-4168; (b) S. J. Marrink, H. J. C. Berendsen, *J. Phys. Chem.* 1996, **100**, 16729-16738; (c) J. M. Diamond, Y. Katz, *J. Membrane Biol.* 1974, **17**, 121-154; dH. Gerhard, *New J. Phys.* 2005, **7**, 34.

[17] (a) J. Aaqvist, A. Warshel, *Chem. Rev.* 1993, **93**, 2523-2544; bH. Lin, D. G. Truhlar, *Theor Chem Acc* 2007, **117**, 185-199.

[18] (a) Z. Shuai, Q. Peng, Y. Niu, H. Geng, *Revision 0.2.004; available online: http://www.shuaigroup.net/, Beijing,China.* 2014; (b) Y. Niu, W. Li, Q. Peng, H. Geng, Y. Yi, L. Wang, G. Nan, D. Wang, Z. Shuai, *Mol. Phys.* 2018, **116**, 1078-1090.